# Influence of the Die Configuration on the Gross Melt Fracture of Linear Polyethylene

**Younggon Son**

*Advanced Materials Science and Engineering, College of Engineering, Kongju National University, Cheonan, Chungnam 331717, South Korea*

Received 27 September 2010; accepted 26 November 2010
DOI 10.1002/app.33836
Published online 29 March 2011 in Wiley Online Library (wileyonlinelibrary.com).

**ABSTRACT:** In this study, capillary extrusion experiments and rupture visualization experiments were carried out with a combined die configuration where two different dies were attached in a capillary rheometer. We observed that the gross melt fracture (GMF) and rupture of the melt occurred simultaneously when the diameter of the die located at the upstream position was larger than that of the die located downstream. However, when the location of the dies were interchanged, that is, the diameter of the upstream die was smaller than that of the downstream die, the upstream rupture did not accompany GMF up to a certain extent of shear rate. From these observations, we present a new theory on the origin of GMF. © 2011 Wiley Periodicals, Inc. J Appl Polym Sci 121: 2812–2817, 2011

**Key words:** polymer extrusion; polymer rheology; polyolefins

## INTRODUCTION

The production rate of extrusion-based processes, such as film blowing, extrusion forming, melt spinning, and cast film extrusion, is limited by defects, such as surface irregularities and melt fracture.[1,2] There are various types of extrusion defects.[1] These defects are often referred to as *flow instabilities* or *melt fractures*, and the defects are classified according to their nature and extrusion rates. At low extrusion rates, an extrudate with a smooth and shiny surface is obtained. As the extrusion rate increases, the extrudate becomes turbid, mat, rippled, and then distorted in a sharkskinlike pattern [sharkskin or surface melt fracture (SMF)]. At higher extrusion rates, the extrudate exhibits alternating smooth and sharkskinned regions along the extrudate axis (stick–slip or spurt flow). Upon further increases in the extrusion rate, the extrudate exhibits more severe and larger distortions [gross melt fracture (GMF) or wavy fracture].

The sharkskinned extrudate generally exhibits regular periodic distortions. It is believed that SMF originates in the die exit region. On the other hand, the gross melt fractured extrudate shows larger irregular distortions and is known to originate from the die entry flow. Considerable effort has been devoted to shedding light on the origins of melt fractures and a more comprehensive understanding has been obtained, especially with regard to SMF.[3,4]

On the basis of these findings, there have been numerous trials to eliminate or delay melt fractures in efforts to realize higher production rates. These include modifications of the die[5,6] and materials by incorporation of processing aids, such as boron nitride,[7] hyperbranched polymers,[8] and fluoropolymers,[9–11] into the base polymer. The use of a slipping agent (fluoropolymer) has thus far yielded the most successful results, and numerous studies have used fluoropolymers.[9–11] Fluoropolymers are known to reduce the extensional force of polymer melts flowing from the die land to the free surface of extrudates near the die exit; they enhance the slippage between the die land and polymer melts. As a result, the fluoropolymer eliminates or delays SMF. However, it does not appear to affect GMF.[11]

Investigations of boron nitride (BN) powder have not fully clarified it effects on melt fracture. Although it appears that BN delays SMF, it has no effect on GMF, except in the case of special dies.[7]

To date, most studies conducted on melt fracture have focused on SMF because it occurs at relatively lower extrusion rates. SMF occurs mostly in linear polymers, such as polydimethylsiloxane,[12] polybutadiene,[3,13] high-density polyethylene, and linear low-density polyethylene (LLDPE). Branched polymers, such as low-density polyethylene, do not show SMF.[14] On the contrary, GMF is observed in most polymers with a high production rate. Nevertheless, GMF has been less actively studied.

*Correspondence to:* Y. Son (sonyg@kongju.ac.kr).

Contract grant sponsors: Korean Ministry of Education, Science and Technology (The Regional Core Research Program/Zero Energy Green Village Technology Center).

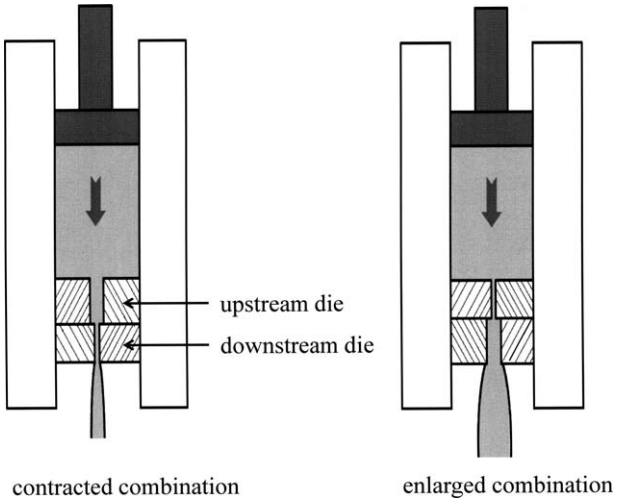


**Figure 1** Schematic diagram of the combined die configuration.

It is known that GMF is initiated at the die entrance region. In efforts to trace the origins of GMF, flow visualization experiments of the die entrance region, where uniaxial extensional flow is dominant, have been extensively used.[15–19] These studies found that the entrance region exhibits a typical converging laminar flow pattern when the flow rate ($Q$) is low. The streamline is continuous, axisymmetric, and time independent at low $Q$ values. As $Q$ increases and reaches a critical value, the converging lamella flow pattern is disturbed, the streamline fluctuates (time dependent), and the axial symmetry of the streamline vanishes. As $Q$ increases further, the melt at the centerline of the entrance region fractures. GMF is always observed to be accompanied by the occurrence of rupture.

Fracture in solids can be thought of as a process that creates new surfaces by external force. *Melt fracture* refers to cohesive failure of a molten polymer when the extensional stress ($\sigma_E$) exceeds a critical stress, beyond which the entanglement between polymer chains cannot be sustained and sudden disentanglement occurs. Because GMF is always accompanied by the occurrence of rupture at the die entrance region, it is believed that the asymmetry and fluctuation propagate to the capillary die and, consequently, result in a chaotic appearance of the extrudates. This behavior is similar to the turbulent flow of a nonelastic liquid. Therefore, GMF is often called an *elastic turbulence.*

In this study, we carried out capillary extrusion experiments with a metallocene-catalyzed polyethylene by a combined die configuration, where two different dies were attached in a capillary rheometer. We documented a very unusual phenomenon at the GMF regime. We observed that GMF was not necessarily accompanied by the rupture of the melts (RM) in some circumstances. In this article, we report these unusual experimental results and suggest a new theory for the origin of GMF.

## EXPERIMENTAL

### Materials

The material investigated was AFFINITY EG8100 (Dow Chemical, Midland, MI), a commercially available metallocene-catalyzed LLDPE. It was characterized by a melt index of 1.0 g/10 min and a density of 0.87 g/cm$^3$ and was copolymerized with 9.8 mol % octene.

### Apparatus and method

Capillary extrusion experiments were carried out with a piston-driven homemade capillary rheometer at a temperature of 140°C. Four different cylindrical steel dies, with an entrance angle of 180° and various length ($L$)/diameter ($D$) ratios (9.3/0.535, 4.56/0.535, and 20.2/1.0 mm/mm), were used. Details of the apparatus were described elsewhere.[11] Flow curves of the LLDPE were obtained from single dies ($L/D$ = 9.3/0.535 and 20.2/1.0) and combined die configurations of two capillary dies, as shown in Figure 1. In the combined die configurations, two different dies were placed one over another. Three different configurations were used. Notation for the die configurations was made as follows. The notation 1.0/20.2UP0.535/9.3DOWN represents a die configuration where a die of 1.0 mm $D$ and 20.2 mm $L$ was placed at the upstream location and another smaller die of $D/L$ = 0.535/9.3 was placed downstream, as shown schematically in Figure 1. Thus, the notation 0.535/9.3UP1.0/20.2DOWN represents the reverse sequence of the same dies of the previous configuration. We also denote a die configuration where $D$ of the upstream die was smaller than that of the downstream die as an enlarged configuration and a die configuration where $D$ of the upstream die was greater than that of the downstream die as a contracted configuration, as shown in Figure 1.

### Upstream rupture visualization

We performed rupture visualization experiments in the capillary rheometer (12-mm barrel $D$). This visualization technique has been used to study entrance flow instabilities by many authors.[15–17] A carbon-black (CB)-filled sample was prepared by extrusion of a mixture of polymer and CB (0.5% mass fraction) into a cylindrical form of approximately 11.5-mm $D$ followed by the cutting of the rod into discs 2 mm thick. Discs of polymer without CB were also prepared in the same manner. The discs were loaded

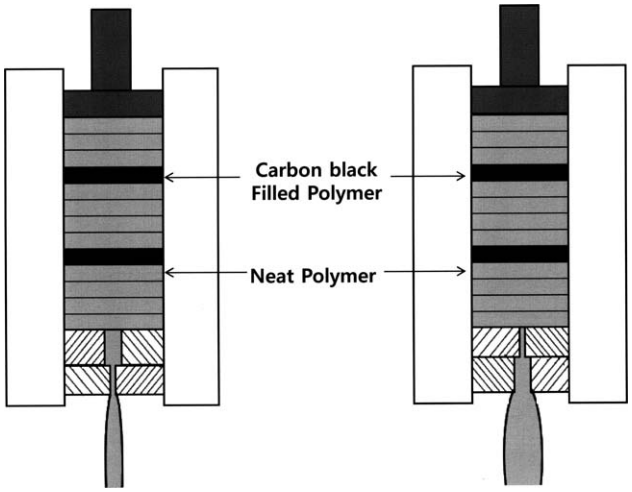


**Figure 2** Method for loading discs into the barrel of the capillary rheometer for the upstream rupture visualization experiment.

into the barrel of the capillary rheometer, which was equipped with a capillary die. One CB-filled disc was inserted at every five polymer discs, as shown in Figure 2. The extrudates obtained from the rupture experiment under various conditions were cut along the axial direction and investigated under an optical microscope in a reflective mode at 2× magnification.

## RESULTS AND DISCUSSION

Figure 3 shows the pressure drop ($\Delta P$) as a function of $Q$ obtained from two single capillary dies and three different die configurations, as described in the Experimental section. Closed symbols represent the

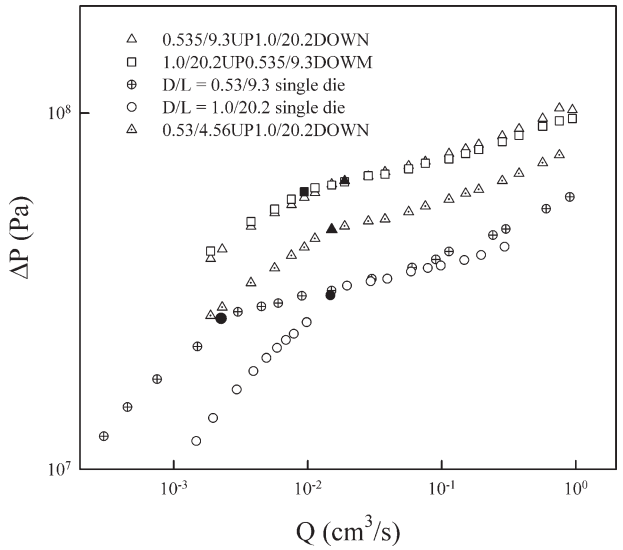


**Figure 3** $\Delta P$ as a function of $Q$ obtained from two single capillary dies and three different die configurations. The filled symbols represent OGMF.

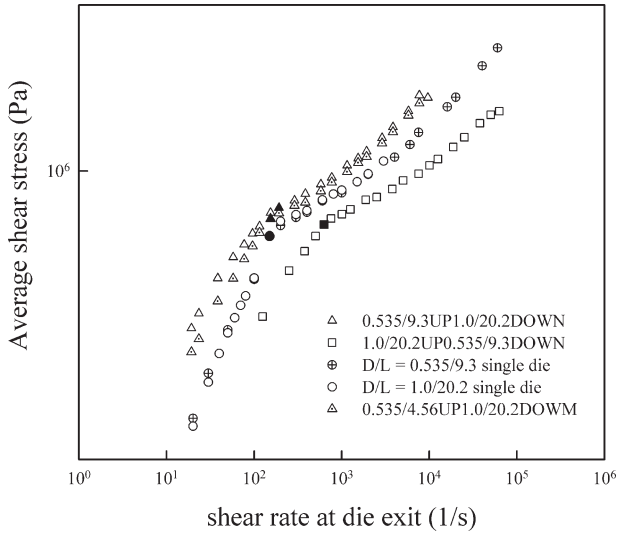


**Figure 4** $\bar{\tau}$ as a function of the shear rate at the die exit. The filled symbols represent OGMF.

onset of gross melt fracture (OGMF). Focusing on $\Delta P$ versus $Q$ obtained from two single dies of $D/L = 0.535/9.31$ and $D/L = 1.0/20.2$, one can see that the critical $Q$ for the OGMF increased with $D$ of the capillary die.

The data shown in Figure 3 were recalculated in the form of shear stress as a function of the shear rate at the die exit and are shown in Figure 4. In the case of the combined die configurations, the average shear stress ($\bar{\tau}$) is calculated as follows:

$$\bar{\tau} = \frac{\Delta P}{2\left(\frac{L_s}{R_s} + \frac{L_b}{R_b}\right)} \tag{1}$$

where $L_s$, $L_b$, $R_s$, and $R_b$ are the lengths and radii of the small die and large die, respectively.

OGMFs for the two different dies overlapped. Another die with a 0.7-mm $D$ exhibited the same onset point with the dies with 0.535- and 1.0-mm $D$ values (not shown in Fig. 4), as shown in ref.[11]. Many studies have suggested that $\sigma_E$ (or tensile stress) at the die entrance region is appropriate as a criterion for OGMF.[15–17] The critical $\sigma_E$ was indeed observed to be independent of the melt temperature and the extensional rate.[15] It appeared that the critical $\sigma_E$ depended only on the material. That is, the critical $\sigma_E$ is an intrinsic property of a given material. The extensional rate and $\sigma_E$ at the die entrance region can be estimated by Cogswell's equation, where the average extensional rate ($\dot{\varepsilon}$) and $\sigma_E$ as a function of end pressure ($\Delta P_{\mathrm{End}}$), apparent shear rate ($\gamma_A$), wall shear stress ($\tau_w$), and power-law index ($n$) are related as follows:

$$\dot{\varepsilon} = \frac{4\gamma_A \tau_w}{3(n+1)\Delta P_{End}} \quad \sigma_E(\dot{\varepsilon}) = \frac{3(n+1)\Delta P_{End}}{8} \tag{2}$$

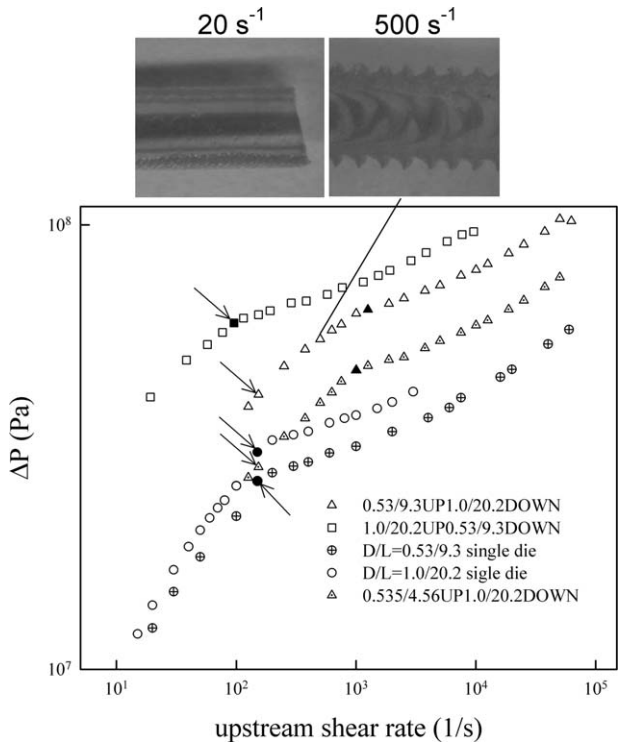


**Figure 5** $\Delta P$ as a function of the shear rate at the die entrance (upstream shear rate). The filled symbols represent OGMF. The data points indicated by arrows represent ORM.

There are several other equations to derive the extensional rate and $\sigma_E$ from $\Delta P_{End}$, $\gamma_A$, $\tau_w$, and $n$. All of the equations show a similar form to that of eq. (2). $\sigma_E$ is a function of the extensional rate and, consequently, $\gamma_A$. According to these equations, the $\sigma_E$ values of two different dies are the same when the $\gamma_A$ values are the same under the same temperature. Therefore, the overlapping of OGMF for different dies in the plot of the shear rate–shear stress is consistent with the findings of previous studies, which concluded that $\sigma_E$ at the die entrance region is a decisive factor for OGMF.[15]

The plot of $\Delta P$ versus $Q$ obtained from different die configurations was unexpected. OGMF for the die configuration 0.535/9.3UP1.0/20.2DOWN was located at a higher $Q$ than that of 1.0/20.2UP0.535/9.3DOWN. This was not anticipated given that the average shear rate (and shear stress) at the upstream die (i.e., the die entrance) for the die configuration 0.535/9.3UP1.0/20.2DOWN was higher than that of the die configuration 1.0/20.2UP0.535/9.3DOWN at the OGMF. Thus, the extensional rate and $\sigma_E$ at the die entrance to die land for the former configuration was higher than that of the latter configuration. These two configurations used the same dies, but their sequence was reversed.

Figure 5 presents $\Delta P$ as a function of $\gamma_A$ of the upstream die (denoted as the *upstream shear rate*), and Figure 6 shows $\Delta P$ as a function of $\gamma_A$ of the downstream die (denoted as the *downstream shear rate*). According to eq. (2), the extensional rate at the entrance region for 0.535/9.3UP1.0/20.2DOWN was higher than that for 1.0/20.2UP0.535/9.3DOWN at the same $Q$ because $\gamma_A$ was inversely proportional to the cube of die $D$: $\gamma_A = 4Q/\pi R^3$. The upstream shear rates for the OGMF were 1254 $s^{-1}$ for 0.535/9.3UP1.0/20.2DOWN and 96 $s^{-1}$ for 1.0/20.2UP0.535/9.3DOWN. It was obvious that the critical extensional rate (consequently, the critical $\sigma_E$) at OGMF for 0.535/9.3UP1.0/20.2DOWN was much higher than that of 1.0/20.2UP0.535/9.3DOWN because $\gamma_A$ of 0.535/9.3UP1.0/20.2DOWN for OGMF was 13 times higher than that of 1.0/20.2UP0.535/9.3DOWN. This was very abnormal and was not consistent with previous studies, which reported that GMF was initiated at the die entrance and that the critical $\sigma_E$ for OGMF was independent of the die size and geometry.

To determine the cause of this discrepancy, a rupture visualization experiment was carried out. Micrographs of selected extrudates for the die configuration 0.535/9.3UP1.0/20.2DOWN are shown in Figure 5. Black lines or black dots inside the extrudates correspond to the portion of CB-labeled polymer (and, thus, a streamline). The micrograph taken at 20 $s^{-1}$ (upstream shear rate) shows that the streamline was very stable and that the outer surface showed a weak sharkskin texture. As $Q$ increased, the SMF became severe and strong. The micrograph taken at 500 $s^{-1}$ shows that the CB-labeled polymer was broken at this point into discontinuous pieces, but the outer surface still showed a typical sharkskin texture, as presented in Figure 5.

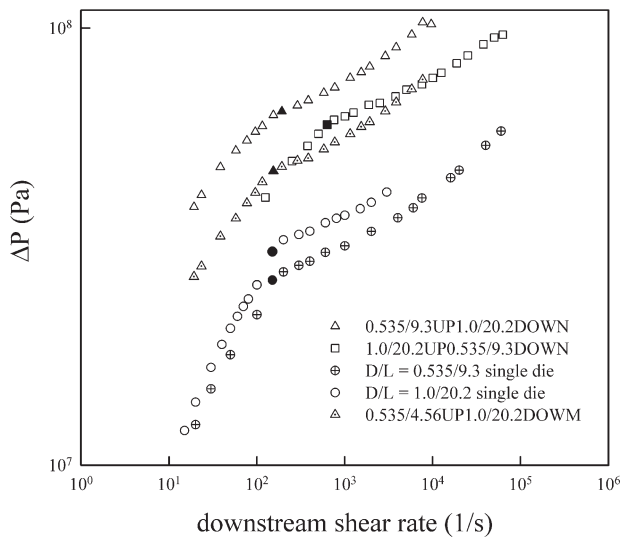


**Figure 6** $\Delta P$ as a function of the shear rate at the die exit (downstream shear rate). The filled symbols represent OGMF.

We believe that this is the first reported observation that RM is not accompanied by GMF. Kim and Dealy[15,16] performed a similar rupture experiment in a capillary rheometer and showed that the GMF was always accompanied by upstream RM. Many other studies have reported the same phenomenon in this respect.[15–19] Therefore, it has long been believed that GMF is initiated by an upstream rupture at the die entrance region.

We determined the onset of the rupture of the melt (ORM) by the rupture visualization experiment, and the onset points are indicated by arrows in Figure 5. Focusing on flow curves of $\Delta P$ versus the upstream shear rate (refer to Fig. 5), one can see that the ORMs were almost at the same upstream shear rate (i.e., the same extensional rate and $\sigma_E$); this implies that the RM started at a critical $\sigma_E$, regardless of the die size and configuration. This is consistent with reported findings. Focusing on flow curves of $\Delta P$ versus the downstream shear rate (refer to Fig. 6) obtained from the single dies ($D/L$ = 9.3/0.535 and 20.2/1.0) and the die configurations 0.535/9.3UP1.0/20.2DOWN and 0.535/4.56UP1.0/20.2DOWN (the enlarged configuration), we observed that GMF started at almost the same downstream shear rate; this implies that the shear rate at the die exit region may have played an important role in GMF. For enlarged configurations, RM occurred at the same critical $\sigma_E$ values with those of single dies, but GMF did not appear up to a certain level of downstream shear rate, even upon RM. The critical downstream shear rate (i.e., the critical shear rate near die exit) at OGMF for the enlarged configurations was observed to be almost the same as those of the single dies. From these experimental results, we speculated that both $\sigma_E$ at the die entrance region and the shear stress near the die exit were decisive factors for GMF. For single dies and the contracted configuration (1.0/20.2UP0.535/9.3DOW), GMF and RM occurred simultaneously; that is, OGMF and the ORM were located at the same shear rate. For the contracted configuration, the downstream shear rate was higher than that of the upstream shear rate at a given $Q$. Thus, once the upstream rupture occurred, GMF occurred simultaneously because the downstream shear rate already exceeded the critical shear rate for OGMF.

From the experimental results presented thus far, we suggest the following theory regarding the origin of GMF. Once RM occurs at the entrance region, the polymer melt possesses a potential GMF. However, if the shear rate near the die exit is not strong enough (or is under a critical value), the ruptured polymer melt does not reveal GMF. GMF occurs only when both $\sigma_E$ at the die entrance region and the shear stress near the die exit are above critical values.

RM starts at almost the same upstream shear rate for a single die and an enlarged configuration. However, for the contracted configuration, ORM starts at a slightly lower upstream shear rate than that of the single die. This is likely because there are two contraction regions for the contracted configuration, that is, one at the die entrance region and another at a region extending from the larger upstream die to the smaller downstream die. Thus, polymer melts flowing through the contracted die configuration experience the extensional force twice, which would likely lower the critical $\sigma_E$ for the ORM.

In this study, we observed very unexpected and meaningful experimental phenomena. In common reported findings, we also observed that $\sigma_E$ at the entrance region was the criterion for the ORM; however, GMF was not necessarily accompanied by RM in some circumstances. We suggest that both $\sigma_E$ at the entrance region and the shear stress near the die exit were decisive factors for OGMF. Furthermore, when looking at OGMFs for a single die of 0.535 mm/9.0 mm and the die configuration 1.0/20.2UP0.535/9.0DOWN, the GMF was delayed to a degree corresponding with roughly a shear rate 5 times higher (i.e., production rate) when a die with $D/L$ = 1.0 mm/20.2 mm was inserted in the upstream position. The insertion of a larger die at the upstream position reduced $\sigma_E$ and, consequently, delayed GMF. This modification of the die configuration increased the total pressure but also considerably increased the production rate to produce the same extrudate in size.

Numerous studies have addressed the issue of delaying GMF. For example, reducing the die contraction angle[20] or placing a filter at the die entrance region[21] can delay GMF to a certain extent. Additionally, there have been trials to modify materials by the addition of a processing aid, such as boron nitride.[7] Although such modifications delay GMF to a certain degree, this study showed a far greater delay of GMF. Additionally, the findings of this study could be used in another extrusion-based process. For example, in an extrusion-forming process, where gas bubbles formed by the blowing agent show instabilities of gas bubbles at the die entrance region due to the highest elongation rate, the instabilities can be avoided by the die configurations suggested by this study.

## CONCLUSIONS

From capillary extrusion experiments conducted with various die configurations, we verified that RM occurred beyond a critical extensional stress at the die entrance region and that this outcome was independent of the die geometries. In a single die or a contracted die configuration, RM and GMF occurred

simultaneously. However, in an expanded die configuration, RM did not necessarily accompany GMF. When $\sigma_E$ at the die entrance region exceeded a critical value, the polymer showed RM. Upon RM, GMF did not occur until the shear stress near the die exit reached a critical value. GMF occurred when both $\sigma_E$ at the die entrance region and the shear stress near the die exceeded critical values.

## References


1. Denn, M. M. Annu Rev Fluid Mech 2001, 33, 265.
2. Hatzikiriakos, S. G.; Migler, K. B. Polymer Processing Instabilities: Understanding and Control; Marcel Dekker: New York, 2004.
3. Inn, Y. W.; Fischer, R. J.; Shaw, M. T. Rheol Acta 1998, 37, 573.
4. Migler, K. B.; Son, Y.; Qiao, F.; Flynn, K. J Rheol 2002, 46, 383.
5. Rutgers, R. P. G.; Mackley, M. R. J Non-Newtonian Fluid Mech 2001, 98, 185.
6. Liang, R. F.; Mackley, M. R. J Rheol 1998, 45, 211.
7. Sentmanat, M.; Hatzikiriakos, S. G. Rheol Acta 2004, 43, 624.
8. Hong, Y.; Cooper-White, J. J.; Mackay, M. E.; Hawker, C. J.; Malmstrom, E.; Rehnberg, N. J Rheol 1999, 43, 781.
9. Migler, K. B.; Lavallee, C.; Dillon, M. P.; Woods, S. S.; Gettinger, C. L. J Rheol 2001, 45, 565.
10. Moynihan, R. H.; Baird, D. G.; Ramanathan, R. J Non-Newtonian Fluid Mech 1990, 36, 255.
11. Lee, H.; Kim, D. H.; Son, Y. Polymer 2006, 47, 3929.
12. Piau, J. M.; El-Kissi, N.; Tremblay, B. J Non-Newtonian Fluid Mech 1988, 30, 197.
13. Zhu, Z. Rheol Acta 2004, 43, 373.
14. Doerpinghaus, P. J.; Baird, D. G. Rheol Acta 2003, 42, 544.
15. Kim, S.; Dealy, J. M. Polym Eng Sci 2002, 42, 482.
16. Kim, S.; Dealy, J. M. Polym Eng Sci 2002, 42, 495.
17. Son, Y.; Migler, K. B. J Polym Sci Part B: Polym Phys 2002, 40, 2791.
18. Bagley, E. B.; Birks, A. M. J Applied Physics 1960, 31, 556.
19. Kazatchkov, I. B.; Yip, F.; Hatzikiriakos, S. G. Rheol Acta 2000, 39, 583.
20. Han, C. D. J Appl Polym Sci 1973, 17, 1403.
21. Goutille, Y.; Guillet, J. J Non-Newtonian Fluid Mech 2002, 102, 19.